MULTIOBJECTIVE OPTIMIZATION IN *Aspergillus niger* FERMENTATIONS FOR SELECTIVE PRODUCT ENHANCEMENTS

Mandal Chaitali, G. K. Suraishkumar[1] and R. D. Gudi

Department of Chemical Engineering
Indian Institute of Technology, Bombay
Mumbai-400076, India

A more comprehensive formulation of optimal control problem to enhance a desired product in a multiproduct fermentation is proposed in this work. Optimal control profiles for multiple substrate additions in fed-batch fermentation of *Aspergillus niger* to maximize either catalase or protease have been developed and experimentally evaluated. The liquid phase oxygen supply strategy (LPOS) has been used to overcome limitations of aeration due to high gas-liquid transport resistance. The optimal control problem involves linearly appearing control variables and the decision space is constrained by state and end-point constraints. The proposed multiobjective optimization is solved by Differential Evolution algorithm, a relatively superior population based stochastic optimization strategy.

Keywords: Bioprocess, Bio-control, Multiobjective optimisation, Stochastic optimisation, Multisubstrate optimisation, *Aspergillus niger*

1. INTRODUCTION

Optimal operation of bioprocesses involving multiple products is required to selectively maximize one product in the space of the minimization of the other products. The application of this multi-objective optimisation in fermentation has not been extensively explored so far, but has been useful in the context of the chemical process application (Kasat et al, 2002). Design of optimal control strategies may involve multiple substrate feeding strategies with state-path and end point constraints.

Differential Evolution (DE), (Storn and Price, 1996) is a stochastic optimisation algorithm and a parallel direct search method, that operates on a population of potential solutions by applying the principle of the survival of the fittest, to produce an optimal solution. It has been used in recent past to solve non-conventional optimization problems involving general constraints (Chiou and Wang, 1999). However, the Differential Evolution strategy has not been applied to solve a multi-objective and multiple substrates feed rate optimization problem. Further, the experimental evaluations of the theoretical strategies are not widely reported.

This work is concerned with the development of optimal control profiles for multiple substrates to maximize one selective product in the space of the minimization of the other product in a multiproduct fed-batch fermentation. The system of focus is the fed-batch fermentation for catalase and protease enzyme production by *Aspergillus niger.* A novel method of oxygen supply through liquid phase H_2O_2 addition has been used for this system with a view to overcome limitations of aeration due to high gas-liquid transport resistance (Sriram et al., 1998).

Email: [1]gksuresh@che.iitb.ac.in

Other substrates that are crucial to the fermentation are the sucrose and nitrogen levels. The problem is bound with the end point constraints to reflect realistic constraints on the final levels of product concentrations. The problem is also typically (upper) bounded by the H_2O_2 level in the fermentation, which is treated in our work as a path constraint. We additionally impose end point constraints to minimize residual levels of substrates at the end of the fermentation. To solve this complex problem we propose the use of the Differential Evolution algorithm. We demonstrate the applicability of the proposed methodology through simulations and experimental validations involving fed batch fermentation of *Aspergillus.* niger.

2. PROCESS MODEL

The production of catalase and protease enzyme by *Aspergillus niger ,* with liquid phase H_2O_2 addition as an alternative source of oxygen, has been chosen as a model system. The models developed are discussed below.

A mass balance for H_2O_2 in the medium, considering that the flux of H_2O_2 in the cell is proportional to the difference of H_2O_2 concentration between the medium and cell, can be written as,

$$\frac{dH}{dt} = \frac{F_H H_{feed}}{V} - \frac{(F_H + F_C + F_N)H}{V} - K_H\left(\frac{4XV}{d\rho} + \frac{\pi d^2}{2}\right)\frac{(H - H_i)}{V} - K_d P_{cat} H \quad \text{.....(1)}$$

A balance on the H_2O_2 concentration, considering the cell as the system, yields the following dynamic balance in terms of the intracellular hydrogen peroxide concentration, Hi,

$$\frac{dH_i}{dt} = K_H\left(\frac{4XV}{d\rho} + \frac{\pi d^2}{2}\right)\frac{(H - H_i)}{V}\frac{\rho}{XV} - \frac{(F_H + F_C + F_N)H_i}{V}$$
$$- KE_i H_i \rho - H_i \mu_m \frac{K_i}{(K_i + H)}\frac{N}{(K_N + N)} \quad \text{.....(2)}$$

The dynamic equation describing cell growth can be written as

$$\frac{dX}{dt} = \mu_m X \frac{K_i}{(K_i + H)}\frac{N}{(K_N + N)} - \frac{(F_H + F_C + F_N)X}{V} \quad \text{.....(3)}$$

The dynamic equation for the catalase production, a growth associated product, is written as

$$\frac{dP_{cat}}{dt} = q_P \mu_m X \frac{K_i}{(K_i + H)}\frac{N}{(K_N + N)}\frac{H_i}{(K_{H_i} + H_i)}\frac{C}{(K_C + C)} -$$
$$\frac{(F_H + F_C + F_N)P_{cat}}{V} \quad \text{.....(4)}$$

The dynamic equation for the protease formation, a non-growth associated product is developed as Luedeking-Piret model

$$\frac{dP_{prot}}{dt} = (a_P \mu_m X \frac{K_i}{(K_i + H)}\frac{N}{(K_N + N)} + b_P X)\frac{C}{(K_C + C)}$$
$$- \frac{(F_H + F_C + F_N)P_{prot}}{V} \quad \text{.....(5)}$$

The mass balances on sucrose and nitrogen concentrations, are represented as:

$$\frac{dC}{dt} = \frac{F_C C_{feed}}{V} - \frac{(F_H + F_C + F_N)C}{V} - Y_{\frac{C}{X}} \mu_m X \frac{K_i}{(K_i + H)}\frac{N}{(K_N + N)}$$
$$- Y_{\frac{C}{cat}} q_P \mu_m X \frac{K_i}{(K_i + H)}\frac{N}{(K_N + N)}\frac{H_i}{(K_{H_i} + H_i)}\frac{C}{(K_C + C)}$$
$$- Y_{\frac{C}{prot}} (a_P \mu_m X \frac{K_i}{(K_i + H)}\frac{N}{(K_N + N)} + b_P X)\frac{C}{(K_C + C)} \quad \text{.....(6)}$$

$$\frac{dN}{dt} = \frac{F_N N_{feed}}{V} - \frac{(F_H + F_C + F_N)N}{V}$$
$$- Y_{\frac{N}{X}} \mu_m X \frac{K_i}{(K_i + H)}\frac{N}{(K_N + N)} \quad \text{.....(7)}$$
$$\frac{dV}{dt} = (F_H + F_C + F_N) \quad \text{.....(8)}$$

Towards obtaining minimal concentration of the substrate and a specific product at the end of fermentation, end point constraints are

$$C(t_f) - C_f \le 0 \quad \text{.....(9)}$$

$$N(t_f) - N_f \le 0 \quad \text{.....(10)}$$

$$P(t_f) - P_f \le 0 \quad \text{.....(11)}$$

End point constraint on the final batch volume

$$V_t - V_f \le 0 \quad \text{..... .....(12)}$$

The sucrose and nitrogen concentrations in the feed and the initial batch volume are treated as decision variables. The lower and upper bound on sucrose and nitrogen source feed are imposed as:

$$C_{feed\,\min} \le C_{feed} \le C_{feed\,\max} \quad \text{.....(13)}$$

$$N_{feed\,\min} \le N_{feed} \le N_{feed\,\max} \quad \text{.....(14)}$$

$$V_{\min} \le V \le V_f \quad \text{.....15)}$$

The variable path is also bounded by a state-path constraint on the level of H_2O_2 in the broth as

$$\frac{H}{X} < 0.005\ mol/g\ of\ cell \quad \text{.....(16)}$$

3. OPTIMAL CONTROL FORMULATION

The objective function is to maximize the final product concentration. Therefore it can be posed as

Max J = P(t_f)…….(17)

Over an assumed value of t_f, N_d discretizations in the time duration [0, t_f] are made and each individual nutrient addition rate is assumed to be approximated by a piecewise constant value. The DE method is a parallel direct search method and it utilizes N_P vectors of decision parameters of dimension ($N_d \times 3$) as a population for each generation, W. The initial population Z_i (i = 1,….N_P) is randomly selected as

$Z_i = Z_{min} + \rho i\,(Z_{max} - Z_{min})$…… (18)

where ρ_i denotes a random number generated from a uniform distribution.

The three main operations in DE are mutation, crossover and evaluation. In mutation, the essential step is generation of the difference vector, D_{jk}, between any two individuals of the N_P vectors. The weighted difference vector is then added to a third randomly selected individual or best performing individual to have a perturbed individual (Storn and Price, 1996) as

$D_{jk} = (Z_j^{W-1} - Z_k^{W-1})$…….(19)

$Z_i^W = Z_P^{W-1} + f\,(Z_i^{W-1} - Z_k^{W-1})$……....(20)

where f ∈(0, 1.2) is a scaling factor .

During crossover, the resulting perturbed individual, Z_i^W from Equation (20) and a target individual in current generation are selected by a binomial distribution to perform crossover operation to generate, an off-spring. In the crossover operation the j^{th} gene of the i^{th} individual at the next generation is produced

from the perturbed individual $Z_i^W=[Z_1....Z_{Nd}]_i^W$ and current individual as $Z_i^{W-1}=[Z_1....Z_{Nd}]_i^{W-1}$

$$Z_{ji} = \begin{cases} Z_{ji}^{W-1} & \text{if a random number} > C_R \\ Z_{ji}^{W} & \text{otherwise} \end{cases} \quad \text{.....(21)}$$

Where j = 1,…N_d, i =1,…N_P and the crossover factor $C_R \in [0,1]$ is a user specified real number.

In DE the evaluation function of an offspring competes one to one with that of its parent (target individual in current generation) and the parent is replaced by its offspring in the next generation only if it is superior than its parent.

In these methods, the penalty terms associated with the violation of constraints are added to the objective function.

$$J[\underline{u}(t)] = P(t_f) + \sum_{l=i}^{I} \varepsilon_l^2 \text{.....(22)}$$

4. RESULTS AND DISCUSSIONS

In all the simulations, the fed-batch fermentation was assumed to start with an initial condition on cell mass (0.75 g l^{-1}), nitrogen source (1.5 g l^{-1}), sucrose (6.0 g l^{-1}), catalase and protease (0.0 g l^{-1}), and H_2O_2 concentration both in the medium and in the cell (0.0 moles l^{-1}). The overall bioreactor run was assumed to be of 30 hours duration and the total run time was divided into 15 intervals of 2 hours duration each, i.e. the value of N_d was assumed to be 15. Thus, in this problem a total number of 49 decision variables were used consisting of 45 decision variables generated from each of the glucose, nitrogen source and H_2O_2 additions, 2 variables for glucose and nitrogen concentration in the feed and 2 variables for initial batch volume and fermentation time. A population of 100 vectors of decision variables in one generation was used i.e., N_P is 100. The initial value of the decision and control variables were determined by using equation (18). A crossover factor (C_R) of 0.5 was used and the program was run for 10,000 generations.

4.1 Optimum run for Catalase Maximization

The results of the catalase maximization are shown in Fig. 1-2. The optimizer predicted that the fed-batch must start from an optimum initial batch volume of 850 ml and optimum nitrogen source and sucrose concentrations in the feed to be 295 g l^{-1} and 300 g l^{-1}, respectively. From this Figure 1, it is clear that the nitrogen source feed additions occur almost in one initial pulse. Whereas, sucrose feed addition is predicted as two initial pulse followed by two end pulse. For H_2O_2 the additions occur over the entire time duration mostly with an increasing profile. As is evident from the results, these profiles are predicted by the optimizer to balance the three effects, viz. those resulting from constraints on final batch volume, the end point residual nutrient and

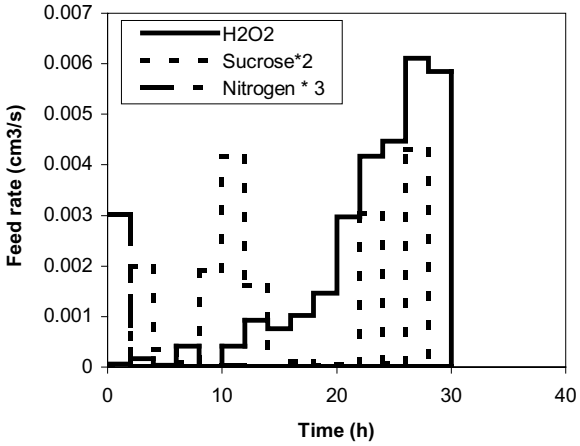

Fig. 1 Optimal feed rate profiles for H_2O_2, sucrose and nitrogen source in catalase maximization run

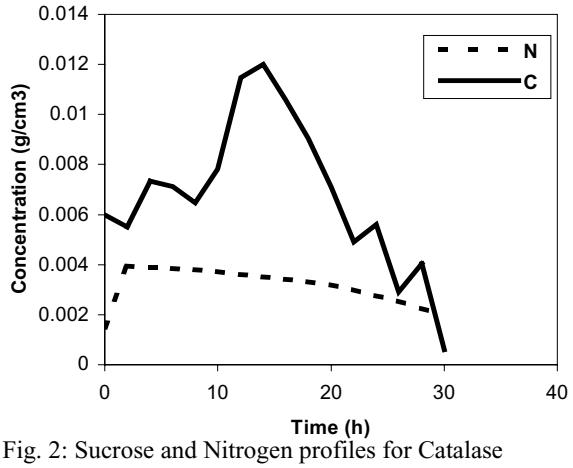

Fig. 2: Sucrose and Nitrogen profiles for Catalase maximization run

protease concentration as well as the nutrient requirements for growth and product formation. A final cell and catalase concentrations of 7.77 g l^{-1} and 4.24 × 10^{-7} M respectively were obtained. The final protease concentration in the catalase maximization run of 5.5 u $^{-1}$l was obtained.

4.2 Optimum run for Protease Maximization

The results of the protease maximization are shown in Fig. 3. In this second case, the optimizer predicted that the fed-batch must start from an optimum initial batch volume of 1250 ml and optimum nitrogen source and sucrose concentrations in the feed to be 300 g l^{-1} and 295 g l^{-1}, respectively. From Fig. 3, it is clear that the nitrogen source feed additions are almost same as catalase run; in one initial pulse. Whereas, the sucrose feed additions are different from that of catalase run; a small initial feed addition followed by an increasing feed rate after 18 hrs of fermentation, to support the non-growth associated protease production, is seen in Fig. 3.

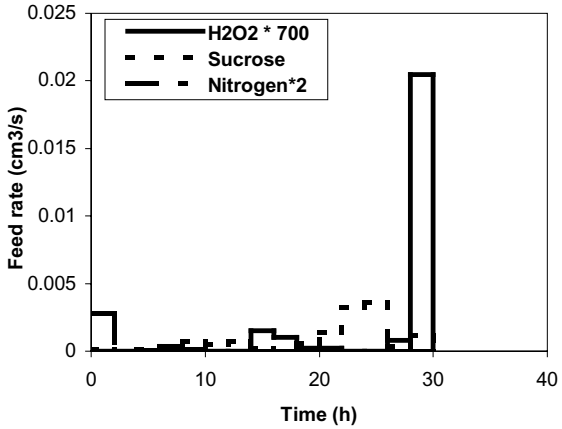

Fig. 3. Optimal feed rate profiles for H_2O_2, sucrose and nitrogen source in protease maximization run

For H_2O_2, the additions occur in a small pulses over the entire time duration with a comparatively large pulse at the end. A final cell concentrations of 12.58 g l^{-1} and a final protease of 7.79 u l^{-1} were obtained. The final catalase concentration in protease maximization run of 3.18×10^{-9} M was obtained.

4.3 Analysis of the optimum runs

The optimal profiles obtained from both catalase and protease maximization are different in nature. The cell mass concentration was found to be higher in case of protease than catalase. The non-growth associated model for protease requires higher cell growth to maximize the final protease concentration. The optimum initial batch volume is lower in case of catalase than protease. In the catalase run there is also a higher dilution due to the continuous addition of H_2O_2. Therefore optimizer recognizes this requirement and predicts a lower initial batch volume for catalase to allow the higher dilution to meet the constraints on the maximum batch volume. In case of protease run the prediction of higher batch volume does not violate the constraint on maximum batch volume. The continuous feed addition profile for H_2O_2 enhanced the catalase production and the pulse addition of H_2O_2 is sufficient to supply the oxygen for cell growth to maximize the protease. The initial and end pulse addition of sucrose is able to maintain an increasing trend of sucrose concentration in the broth, shown in Fig. 2. to support the growth associated catalase production, followed by a decrease in sucrose concentration to meet the minimum residual concentration at the end of the fermentation. On the other hand there is initially small addition of sucrose followed by an increasing feed addition to support the non-growth associated protease production.

4.4 Analysis of the other simulation results

Different runs

1. Optimal run for catalase maximization with end point constraint on sucrose and nitrogen.
2. Catalase Max. without any end point constraint
3. Catalase Max with end protease upwards than the optimal threshold value
4. Catalase Max with end protease down wards than the optimal threshold value
5. Optimal run for protease maximization
6. Protease Max. without end point constraint
7. Protease Max with end catalase upwards than the optimal threshold value
8. Protease Max with end catalase down wards than the optimal threshold value

The results obtained from different simulations are presented in Table 1.

Table 1: Final concentration obtained from different simulations

Run	X (g/l)	Catalase (mole/l)	Protease (units/l)	Nitrogen (g/l)	Sucrose (g/l)
1	7.8	4.24×10^{-7}	5.53	1.99	0.6
2	8.2	4.48×10^{-7}	5.78	8.2	0.3
3	8.5	4.11×10^{-7}	6.0	1.99	0.6
4	4.1	3.04×10^{-7}	2.8	1.99	0.6
5	12.6	3.18×10^{-9}	7.79	1.99	0.9
6	13.2	1.63×10^{-11}	8.21	8.50	2.9
7	12.6	3.52×10^{-7}	4.92	1.99	0.9
8	12.6	1.47×10^{-9}	7.77	1.99	0.6

Effect of end protease concentration in catalase maximization

In catalase maximization, Run 3, the specification of a higher final protease concentration than its threshold optimal value decreases the final catalase concentration from its optimal value. This is because the enhancement of one product in a multi-product fermentation, simultaneously decrease the concentration of the other product to maintain the material balance. In Run 4, the decrease in protease concentration than its threshold optimal value should increase the final optimal catalase concentration. But Run 4 shows a lower value of final catalase than its optimal value. The reason for this behaviour is that, the end point constraint to lower down the final protease concentration from its optimal threshold value directed the optimizer towards the low cell mass production. Therefore catalase production being a growth associated product decreased from its optimal value by this low cell concentration.

Effect of end catalase concentration in protease maximization

In case of protease maximization, Run 8, the specification of a lower final catalase concentration from its optimal value directed the optimizer towards a decrease in the cell concentration. As an effect of this

decrease in the cell concentration, the final protease concentration also decreases from its optimal value, though the change in the final concentration is almost negligible. On the other hand the end point constraint to up wards the final catalase concentration, Run 7, from its optimal value decreases the protease concentration from its optimal value. Therefore we can say that the enhancement of one product reduced the concentration of the other product to maintain the mass balance in the competitive substrate utilization system.

End Point Constraints on the Final Residual Nutrient Concentrations

One of the other interesting aspects of this work is the reduction of the final residual nutrient concentrations by applying end point constraints on them; this has been proposed here to ease separation during downstream processing. The optimization problems without imposing any end point constraints on the final residual nutrient concentration, Run 2 and Run 6, yields a high residual nutrient concentration at the end of the fermentation that could interfere with the downstream processing. It shows a high residual nitrogen concentration of 8.2 gl^{-1} (run 2) and 8.5 gl^{-1} (run 6) at the end of the fermentation when there is no end point constraint imposed on residual nitrogen. On the other hand in case of the optimum (Run 1 and 5) a very low residual nitrogen concentration of 1.99 gl^{-1} is obtained for both the run. This indicates a trade-off between high final concentrations of the product and the residual nutrient levels. Relaxation of the end-point constraints could yield higher final product concentrations but at the expense of higher residual nutrient levels which translate to higher processing/downstream costs.

State-Path Constraints on Nutrient Additions

As stated above in equation (16), a state-path constraint is used in this optimization problem to bound the toxic level of H_2O_2 concentration on the cell growth. The results obtained are presented in Fig. 4. It shows that the H/X value was maintained below the threshold value of 0.005 mol/g-cell over the entire duration of fermentation.

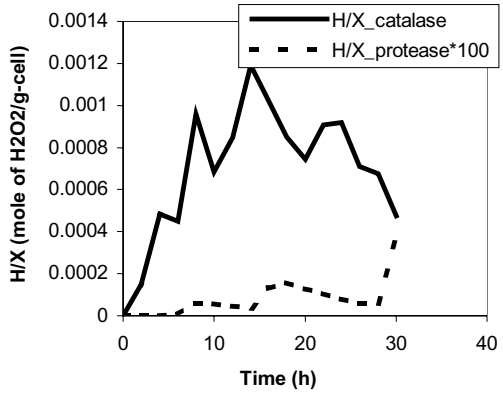

Fig 4: Profiles of the constraint, H/X

4.5 Experimental Evaluation of the Simulation Results

Catalase Maximization

The catalase and the cell concentration profiles obtained from the simulation results have been validated here through experiments shown in Fig 5 and 6. It was observed that the experimental results were broadly in agreement with the simulation results. A final cell concentration of 7.28 g l^{-1} obtained from the experiment compares reasonably well with 7.77 g l^{-1} from simulations. Also the catalase concentration of 2.65×10^{-7} M from experiments, at 28 hours of fermentation, is also comparable with than of 3.61×10^{-7} M form simulation, at 28 hours. A 70% higher catalase than batch cultivation with constant feeding of H_2O_2 at 12 ml h^{-1} was predicted by the optimiser and realised experimentally.

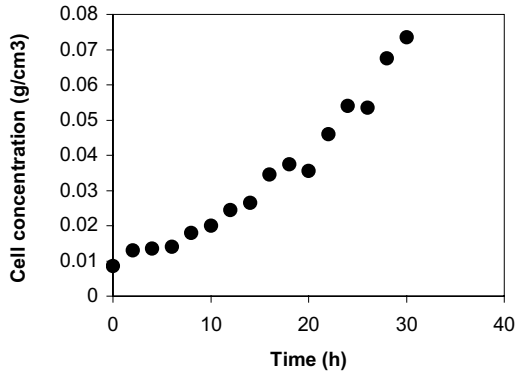

Fig 5: Cell concentration profiles from experimental results for catalase maximization

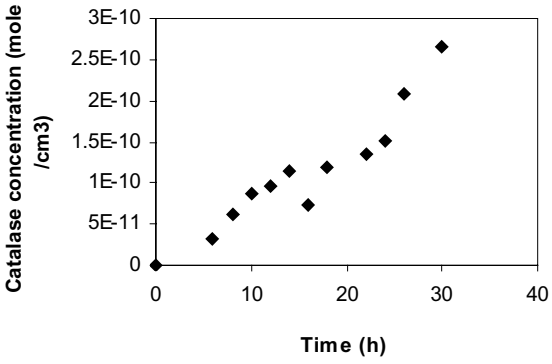

Fig 6: Catalase profiles from experimental results for catalase maximization

Protease Maximization

The product and the cell concentration profiles obtained from the simulation result have been validated here through experiments shown in Fig. 7 and 8. It was observed that the experimental results were broadly in agreement with the simulation results upto 17 hours of fermentation. After that the

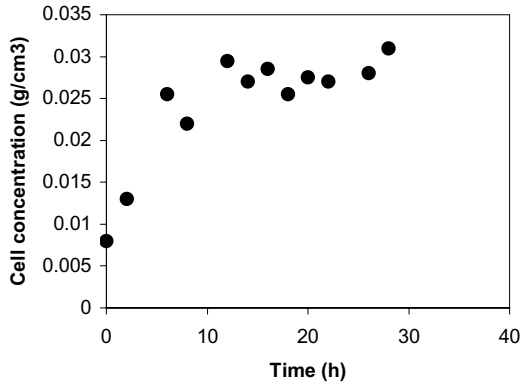

Fig 7: Cell concentration profiles from experimental results for protease maximization

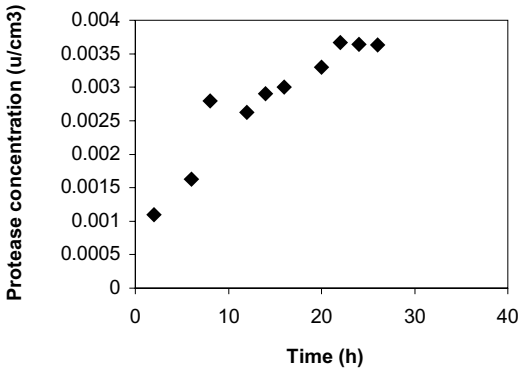

Fig. 8: Protease profiles from experimental results for protease maximization

experimental growth profile follows the stationary phase whereas the simulation result follow the exponential growth due to exponential growth model. A prolonged stationary phase of 18 hours and a final cell concentration of approx 3.1 g/l were obtained from the experiment. A final protease concentration of 3.7 u l^{-1} was obtained. A 31% higher protease than batch cultivation with constant feeding of H_2O_2 at 12 ml h^{-1} was obtained.

5. CONCLUSIONS

This article proposed a more complete formulation of the optimal control problem for multiobjective optimisation in fed-batch fermentations. The formulation proposed an inclusion of end point and state-path constraints to pose the fed-batch fermentation requirements more realistically. A robust stochastic optimization algorithm based on differential evolution was found to solve the resulting optimization problem. The results obtained from simulations were verified experimentally and showed an increase of about 70% and 31% final product concentration compared to conventional batch cultivation.

6. NOMENCLATURE

E_i	intracellular enzyme (2.23×10^{-13} mole cm^{-3} g^{-1})
F_H	hydrogen peroxide feed rate ($cm^3 s^{-1}$)
F_C	sucrose feed rate ($cm^3 s^{-1}$)
F_N	nitrogen source feed rate ($cm^3 s^{-1}$)
K	rate constant (7500000 $(mole\ cm^{-3})^{-1} s^{-1}$)
K_H	H_2O_2 permeability across the cell (0.812×10^{-7} cm s^{-1})
K_{Hi}	Monod type constant (5×10^{-7} mole cm^{-3})
K_N	Monod type constant for nitrogen (1.4×10^{-4} g cm^{-3})
K_C	Monod type constant for sucrose (0.3×10^{-4} g cm^{-3})
K_i	inhibition constant for H_2O_2 (0.24×10^{-4} mole cm^{-3})
q_P	catalase yield (mol catalase (13.26×10^{-9} g mass)$^{-1}$)
a_P	protease yield (0.044 unit protease (g mass)$^{-1}$)
b_P	protease yield with respect to maintenance (5.43×10^{-7} unit protease (g mass)$^{-1}$ s^{-1})
d	diameter of the hyphae (13.43 cm)
ρ	density of the hyphae (1.02 g cm^{-3})
$Y_{N/X}$	inverse of cell yield with respect to nitrogen (0.015)
$Y_{C/X}$	inverse of cell yield with respect to sucrose (0.68)
$Y_{C/Pcat}$	inverse of catalase yield with respect to sucrose (1.01×10^{8})
$Y_{C/Pprot}$	inverse of protease yield with respect to sucrose (8.54)
V_f	max. working reactor volume (1.4 l)

Greek Letters

μ_m	maximum specific growth rate (2.77×10^{-5} s^{-1})
ε	penalty factor

REFERENCES

Storn, R. and K. Price (1996). Minimizing the real functions of the ICEC'96 contest by differential evolution. *IEEE Conference on Evolutionary Computation*, **Nagoya**, 842-844.

Sriram, G, Y. ManjulaRao, A.K Suresh and G.K Sureshkumar (1998). Oxygen supply without gas-liquid film resistance to *Xanthomonas campestris* cultivation. *Biotechnol. Bioeng.*, **59**: 714-723.

Chiou, J.P and F. S. Wang (1999). Hybrid method of evolutionary algorithms for static and dynamic optimization problems with application to a fed-batch fermentation Process. *Comput. Chem. Eng.*, ***23***, 1277-1291.

Kasat, R. B, D. Kunzru, D. N. Saraf and S. K. Gupta (2002). Multiobjective optimisation of Industrial FCC Units Using Elitist Nondominated Sorting Genetic Algorithm . *Ind. Eng. Chem. Res.*, **41**, 4765-4776.